# Evidence of quantum confinement effects on interband optical transitions in Si nanocrystals

M. I. Alonso,[*] I. C. Marcus, M. Garriga, and A. R. Goñi
*Institut de Ciència de Materials de Barcelona, CSIC, Esfera UAB, 08193 Bellaterra, Spain*

J. Jedrzejewski and I. Balberg
*The Racah Institute of Physics, The Hebrew University of Jerusalem, Jerusalem 91904, Israel*
(Received 31 March 2010; revised manuscript received 9 June 2010; published 1 July 2010)

We present evidence for quantum confinement effects on optical transitions in ensembles of Si nanocrystals (NCs) in a $SiO_2$ matrix by considering simultaneously the dielectric function dispersions obtained by spectroscopic ellipsometry, the absorption edge, and the photoluminescence. We find that all these quantities blueshift in a similar manner with decreasing size of the NCs for diameters $d$ below 6 nm. The correlated behaviors of the three observed optical transitions, the optical gap $E_G$, and the critical points $E_1$ and $E_2$, indicate conclusively that their measured blueshifts are associated with the same quantum confinement effect and that the "entire" band structure shifts with $d$. In addition, our results show that the features of the band structure of Si NCs in the $d > 4$ nm range are qualitatively similar to those of bulk Si. In particular, the indirectlike nature of the band gap and the criticality of the L and X points of the bulk Brillouin zone are retained, on the understanding that these concepts cannot be strict in nanocrystals of small dimensions.

## I. INTRODUCTION

While very many spectroscopic ellipsometry studies were carried out on samples containing Si nanocrystals (NCs), the evidence of quantum confinement (QC) effects on optical transitions beyond an energy of $h\nu = 3$ eV is not very convincing. In particular, the correlation between these higher-energy transitions and the more commonly studied optical processes, the band-gap absorption and the photoluminescence (PL), have not been reported. Most of previous works were either concerned with the sample-film properties as such[1–7] or with systems that are essentially hydrogenated microcrystalline Si ($\mu$c-Si:H),[8,9] where QC effects are not expected to be observed. In the systems where the latter effect has been claimed, it was usually concluded essentially for one size of the NCs and the comparison was made with the dielectric functions of the bulk.[10–12] An approach that yielded an indication of the blueshift of the electronic interband transitions, i.e., critical points (CPs) $E_1$ and $E_2$, was recently reported for Si thin films, but the blueshift was extremely small (on the order of the thermal energy).[13] Also no comparison was made there with the corresponding behavior of the PL or the absorption edge. On the other hand, another study of very thin silicon films[14] revealed well the blueshift of the absorption edge but the smearing of the dielectric functions did not enable any conclusion regarding the energy shift of the upper transitions. The only previous trial to make a more comprehensive study[15] was carried out on samples where the PL had shown a weak QC effect but the absorption and dielectric functions data were blurred so that no solid conclusion could have been drawn. In short, the detection of the QC effect beyond the band gap in Si NCs was not really discernible previously and its evaluation is long called for. A particularly interesting but unanswered question is the relation between the PL and the absorption edge concerning the large energy separation between them. The energies of PL and absorption may show a common variation, as expected from the simplest models of QC,[16,17] or the PL may be much

less sensitive to the QC when surface states are involved as discussed by Wolkin *et al.*[18] for porous Si. It was shown[19] only quite recently that the PL can be due to either one of these mechanisms in some Si NCs but it is not clear *a priori* which one is applicable to systems of $NCs/SiO_2$ composites such as those studied here.

Research on silicon nanostructures has been continuously stimulated by the possibility of light emission with tunable energy and usable efficiency at room temperature in spite of the indirect nature of the fundamental gap. For this purpose it is crucial to understand the physical effects of reduced dimensionality on the electronic band structure of Si. For a review see Ref. 20. In particular, the determination of the complex dielectric function $\varepsilon(\omega) = \varepsilon_1(\omega) + i\varepsilon_2(\omega)$ using spectroscopic ellipsometry allows us to obtain important device design parameters such as the index of refraction in the transparent region and the energies of the CPs. The importance of this subject has motivated a number of investigations, both experimental[1–14,21,22] and theoretical.[23–25] However, there are considerable discrepancies and even contradictory results. Among these results, the phenomenology of ultrathin films or nanoslabs[7,13,14] seems better established but the evolution of the band structure of Si nanocrystals as a function of nanostructure size remains unsettled: the most complete experimental reports that considered the NC size are those by Gallas *et al.*[21] and Ding *et al.*,[22] which show contradictory results. Moreover, they did not study the effect of confinement on the CP energies.

The motivation of our work is to shed light on the issues of quantum confinement and critical points, solving these contradictions. We actually follow the optical transitions as a function of NC diameter $d$ and correlate their energies with those of optical absorption and PL that were obtained in parallel. An important advantage of our samples is that they have been previously characterized for both the NC Si content[26,27] and the corresponding NC sizes[16,28,29] so that these parameters can be reliably used in the determination of the dielectric functions. The other important advantage is

that the transition energies are presented here explicitly as a function of the NC sizes enabling us to find semiquantitative trends for the QC effect. In turn, the latter results can serve for future band-structure calculations with the confidence that the QC effect, in transitions with higher energy than the band gap, is the same as the one that is reflected by the commonly available PL data. In our study we were able to achieve all that by taking advantage of the sample deposition by the cosputtering technique that enables the generation of Si NCs of various sizes under the same conditions.[26,28,29] The other advantage is that by using the clearly immiscible phases of Si NCs and $SiO_2$ we avoid the data smearing by the amorphous Si phase, that was found to blur the results when microcrystalline Si deposition techniques are applied.[6,14]

In this study we investigate then a set of samples with rather spherical Si NCs embedded in a $SiO_2$ matrix.[29] We follow systematically the absolute value and spectral dependence of $\varepsilon(\omega)$ as a function of the Si NC diameters between 4 and 8 nm, which turns out to be a size range where quite large changes are detected. Regarding the absolute value of $\varepsilon(\omega)$, we find a very large reduction in the static dielectric constant (i.e., long-wavelength) $\varepsilon_1$, which we discuss and compare with previous literature results. However, our main interest in the present work is the spectral dependence of $\varepsilon(\omega)$ and especially the observation of QC effects on the interband transition energies. In our study we were able to determine $\varepsilon(\omega)$ by a numerical fit without imposing any dispersion law *a priori*. This allows us to perform an accurate analysis of the CP transition energies $E_1$ and $E_2$ and to relate the corresponding QC effects to those revealed by the blueshift of the absorption edge, $E_G$, and the blueshift of the PL. The structure of the paper is as follows: in Sec. II we describe briefly the sample preparation, characterization and optical studies as those were given in detail in previous papers. Since PL results were published elsewhere,[26] we elaborate in Sec. III only on the ellipsometry and optical transmission studies. In Sec. IV we discuss the new findings and the comprehensive picture that emerges from the integration of all our previous and present data.

## II. EXPERIMENTAL DETAILS

The films used in this study were prepared by RF cosputtering from two separate sources (targets), 5 cm in diameter each, such that their centers were 15 cm apart. One target consisted of high purity (99.999%) sintered silicon pellets and the other was pure (99.995%) fused quartz. The substrates were typically 13-cm-long, 1-cm-wide, and 0.7-mm-thick quartz slides. For the sputtering process the slides were positioned 6 cm above the line connecting the centers of the two targets and parallel to it. The deposition conditions were similar to those used in the studies of granular metal systems[30,31] and in other works on Si-$SiO_2$ composites. The thickness of the cosputtered films was about 1 $\mu$m, typically obtained after a couple of hours of cosputtering.

The Si phase content, which varied along the Si substrate, was determined using separate depositions of the Si phase from one source and the $SiO_2$ phase from the other source onto reference substrates. Then, the thickness of the deposited layer, Si or $SiO_2$, was used to evaluate the composition of the cosputtered Si-$SiO_2$ layer (volume percent of the Si phase embedded in the matrix of the $SiO_2$ phase, $x$). Using the well-known method suggested for this purpose[30,31] we found[27] that, over the 13 cm substrate, the Si volume fraction varied from 5% to 94%. After deposition, the samples were annealed at 1150 °C for 40 min to form Si NCs in the $SiO_2$ matrix. The nanostructural properties of samples prepared under these same conditions have been previously characterized[16,26–29] using several techniques showing that the material is a nanocomposite of rather spherical NC-Si and $SiO_2$. The sizes of the NCs were evaluated by high-resolution cross-sectional transmission electron microscopy (HRTEM).[28,29] The size distributions as reflected by the size histograms reported in Refs. 16 and 28 are relatively narrow with peak values between 3 (Refs. 16 and 32) and 15 nm,[29] depending on the content of Si and $SiO_2$ at each spot. Since all samples have been generated in a same high-temperature annealing, all NCs are highly crystalline and the composite material is compact, without pores. The cosputtering and the annealing processes were always carried out on two parallel substrates simultaneously so that a variety of measurements (notably PL and transport[29]) could be carried out on essentially the "same" sample. Our very many pairs of samples that have been measured, in particular their PL (that was our main characterization tool[16,26,32]), have shown the same spectra. In fact, samples prepared in different runs under "identical" sputtering and annealing conditions did not show any significant variations in their properties in general and the PL, in particular. For the present study one sample (Si-$SiO_2$ layer) was used for the ellipsometry and optical transmission studies while its twin was previously used for the PL (Refs. 16 and 26) and the HRTEM (Refs. 16 and 28) studies.

The first optical characterization tool of the samples was the dependence of the PL spectra on the Si fractional volume content $x$, as described in great detail previously.[16,26,29,32] The PL was measured with the 488 nm excitation from air-cooled or water-cooled Ar-ion lasers. The typical irradiation flux from either source was on the order of 10 W/cm². In the first laser setup,[29] the detection was done with an optical fiber that led the luminescence directly to the spectrometer (Control Development Inc.), whereas in the other setup, the PL signal was dispersed by a 250 mm spectrometer onto a photomultiplier that fed a photon-counting system.[16,26,32] Ellipsometry and transmission measurements were performed at room temperature using as basic optical setup a rotating polarizer SOPRA ES4G spectral ellipsometer. The light source was a 75 W high-pressure Xe arc lamp and the reflected or transmitted light was collected by an optical fiber and could be analyzed in two different detection setups. From 0.7 to 1.4 eV the spectra were measured by using a single spectrometer of 300 mm focal length and a Peltier-cooled GaInAs photodiode. From 1.4 to 5.2 eV we used a double prism/grating monochromator of 750 mm equivalent focal length and a multialkali photomultiplier tube. Complementary Raman measurements were taken using Ar-ion laser excitation (514 nm line) and a LabRAM HR system for de-
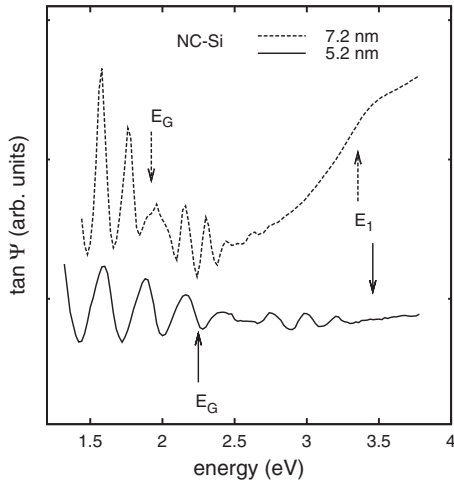
FIG. 1. Detail of the as measured tan $\psi$ spectra for two of the samples. The two observed onsets of absorption attributed to the optical band gaps $E_G$ and the $E_1$ transitions are indicated in the figure. The arrows indicate the energies obtained from transmission measurements ($E_G$) and from the fitted dielectric functions of nanocrystals ($E_1$). The vertical scales have been arbitrarily displaced for clarity but the units of both curves are the same.

tection. Also, for completeness, we measured both the as-deposited and the annealed samples.

The ellipsometric measurements on the as-deposited samples showed very broad and featureless spectra. On the contrary, the optical response of the annealed samples contained well-defined peaks, characteristic of crystalline materials, especially in the Si-rich end of the elongated sample. The Raman measurements supported this behavior by showing for the Si-rich end of the annealed samples, where no PL is observed,[29] the presence of Si NCs with estimated sizes around 15 nm, in good agreement with our above-mentioned HRTEM results. However, the Raman signal toward the Si-poor end was quite weak and even masked by the intense photoluminescence. No signature of amorphous Si phase was detected in the annealed samples.

## III. RESULTS AND ANALYSIS

### A. Derivation of the dielectric functions

The ellipsometry measurements consist in detecting the change in polarization state of light reflected on the sample surfaces, which is given by the complex reflectance ratio $\rho = \tan \Psi e^{i\Delta}$. Each measurement determines the amplitude, $\tan \Psi$, and the real part of the phase shift, $\cos \Delta$. From spectra of these ellipsometric parameters we deduced the sample properties of interest.[33] By mere inspection of the raw ellipsometric spectra we can see some relevant features. For example, in Fig. 1 we display results of two measurements of $\tan \Psi$ for two different sizes of the NCs. At lower energies, the films are transparent and we observe interference oscillations. The sudden amplitude reduction in these oscillations indicates an absorption onset.[34] We observe two such onsets very clearly, not only in these but in all spectra of NCs larger than $\sim 5$ nm. The first optical band gap $E_G$ displays a strong
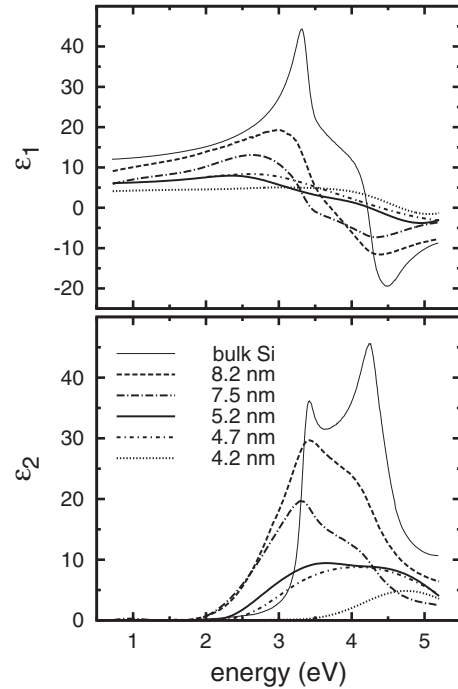


FIG. 2. The dielectric functions of our NC-Si ensembles for crystallites of different average sizes. The nanocrystals were embedded in a SiO$_2$ matrix but the contribution of the oxide is already taken into account by the effective-medium model described in the text. Therefore, the displayed evolution corresponds to the crystallites only.

blueshift as the NCs become smaller. But it is not obvious from the raw data where to place the transition energies, therefore we will refer to the determination of these energy values in the next section (Sec. III B).

In general, spectra are analyzed by numerical procedures based on a model of the sample structure including the substrate and film properties such as film thickness and dielectric function. The numerically deduced dielectric functions shown in Fig. 2 illustrate clearly the overall change that occurs for NCs between 4 and 8 nm: above the NC size of $\sim 5$ nm the dielectric function of the crystallites is reminiscent of the bulk with broad but clear $E_1$ and $E_2$ energies of the CPs. Below this size, the $E_1$ transition becomes quite broad and weak and tends to disappear. The remaining broad structure for smaller NCs seems related then to $E_2$.

The dielectric functions shown in Fig. 2 correspond to Si NCs and are obtained by fitting the spectra with a four-phase model (ambient/rough overlayer/EMA layer/substrate), where the effective-medium approximation (EMA) layer is composed of a SiO$_2$ matrix and NC Si particles for which the dielectric function is not known. The rough overlayer is introduced as usually by an EMA mixture of the material and voids.[35] All considered effective media consist of isotropic particles embedded in a self-consistently determined background. Therefore, the model is valid in the full range of compositions. We mention that the actual equations used for the fitting consider dipole averaging in order to determine the self-consistent background medium.[36] While, *a priori*, this detail is not relevant for the results presented below since we

are dealing with spherical particles, the algorithm would allow to consider other particle geometries, if necessary.

The variable parameters of the used model were: the layer thickness and its composition (i.e., volume fraction of each component), as well as the unknown dielectric function of the Si NCs that had to be determined. We fixed the thickness of the surface roughness to 2 nm and the volume fraction of surface voids to 0.5 for all cases. To optimize the variable parameters we made two successive steps.

First, we determined all layer thicknesses by fitting an unknown effective layer using reference values of the quartz substrate dielectric function. The unknown film dielectric functions were parametrized using splines, as described elsewhere.[33] This general parametrization is very useful to fit layer thicknesses in the same way for all samples, without having to introduce explicit models for the different layers which, in principle, may be different. The thicknesses obtained for these films were around 1.2 $\mu$m, being thicker for the Si-rich end of the film than for the $SiO_2$-rich end, but pretty constant in the intermediate silicon content region that is of concern here. In this region we find, with increasing Si content, NC diameters between 4.0 and 7.5 nm. Once the layer thicknesses are known, we repeated the fits by using explicitly an EMA layer with a $SiO_2$ reference as one of the components, which allowed us to obtain from the fits an optimum $SiO_2$ content and a fitted dielectric function of the NC-Si for each spectrum. Dielectric functions have been obtained both as splines and from energy-by-energy numerical inversion, noting that the latter is the more accurate numerical solution for the determination of the transition energies (Sec. III B).

The compositions obtained by this procedure were very close to those obtained from calibrations made on the basis of the above-mentioned cosputtering geometry[30,31] and other characterizations.[27] The present fits yielded an estimated error of $\pm 5$ vol %. From the previous detailed determination of the $d(x)$ dependence in these samples the average NC diameter can be described by $d \sim 2(x-x_0)^{1/3}$, where $d$ is in nanometer and $x_0=8$ vol %.[16] Utilizing the established compositions we assigned then the NC sizes by using this relationship. The error in the determination is largest for the smallest nanocrystals and thus we estimate, from the fit uncertainties, errors on the order of $\pm 1$ nm.

The absolute values of the dielectric functions shown in Fig. 2 obviously tend to decrease strongly when the NC sizes decrease. This reduction compared to bulk material has been reported before for other types of samples containing NC-Si.[10,37] In those works, however, only NCs around some particular average size were studied and the progressive reduction with size was not addressed. The decrease in the dielectric functions was also reported in ultrathin μc-Si:H films[14] and recently, studied as a function of thickness in nanoslabs.[7] In the latter case, the reduction in $\varepsilon_1$ as compared to the bulk value was found to be on the order of 13% at 0.73 eV in 3.3-nm-thick slabs, which is noticeable, but small compared to other reported values. For example, about 25% reduction was reported for 3.3 nm nanocrystals.[10] Here we found even larger reductions. As noted in Ref. 7, the expected reduction is strongly dependent on the nanostructure shape, and it is qualitatively expected that we find a smaller absolute value for spherical nanodots compared to the more elongated shapes such as slabs or disks.

Concerning the reduction in $\varepsilon_2$, our results are comparable to the results reported by Ding *et al.*,[10] but they have studied only NC sizes between 3.3 and 4.6 nm and not all samples underwent an annealing process. On the contrary, we investigated a wider range of sizes which were generated under the same annealing conditions (the crystallinity as noted above is complete in all our annealed samples.)

Concerning the spectral behavior, our observations are also similar to those of Ding *et al.*[10] In their case, a reduction of $\sim 1$ nm in size implied a complete qualitative change in the spectral shape, changing from a bulklike spectrum to a broadened function. In our NCs, the size where this transition occurs is larger than in their study, about 5–6 nm, which is around the size for which the number of atoms in the volume is about the same as at the surface of the crystallite and the surface effects start to dominate the bulk effects. Noticing that the electronic states and the polarizability are highly susceptible to surface conditions, this can explain that the reduction is larger for systems with more surface-to-volume ratios, i.e., for spherical nanoparticles. This effect is most likely the reason for the much stronger reduction observed in our NC-Si spheres below a diameter of 6 nm.

### B. Electronic transition energies

Concerning the band to band transition energies, the most studied issue in the past has been the observation of a well-defined absorption onset or "optical gap" $E_G$ that blueshifts strongly with decreasing size of the NCs. Although it is not clear yet if NC-Si is a direct gap system, its oscillator strength is far stronger than that characterizing the indirect transition in bulk c-Si and seems to evolve from it as a result of quantum confinement.[14,23–25] As for the upper transitions, the only previous systematic study[13] was carried out in nanoslabs, where the dielectric functions remain "bulklike" down to $\sim 3$ nm slab thicknesses.

To determine the energy $E_G$ of the optical gap that was already apparent in the ellipsometric spectra shown in Fig. 1, we have measured the transmission of some representative samples. Depending on the size and concentration of the NC-Si and the film thickness, we got, as shown by the experimental points in Fig. 3(a), transmitted light up to different energies for different samples, allowing us to calculate the absorption $\alpha$ in a limited energy range as $\alpha \propto [-\log(I/I_0)/x\ell]$, where $I/I_0$ is the transmitted fraction of light, $x$ the Si concentration, and $\ell$ the film thickness. The function $(\alpha h\nu)^{1/2}$ plotted as function of $E=h\nu$ has a linear behavior in the considered energy range. The extrapolation to $\alpha=0$ by a least-squares fit gives an optical gap energy, as illustrated in Fig. 3(a). Despite the somewhat large scatter of the data points, it is obvious that the gap shifts toward higher energies when the NC size decreases. Part of the scatter in the results may be due to the restricted spectral range of $\alpha$ available for the extrapolation, which varies from sample to sample. In a crystalline material values closer to $\alpha=0$ should be considered to obtain the band gap. We can do that by using the dielectric functions shown in Fig. 2 and consider-
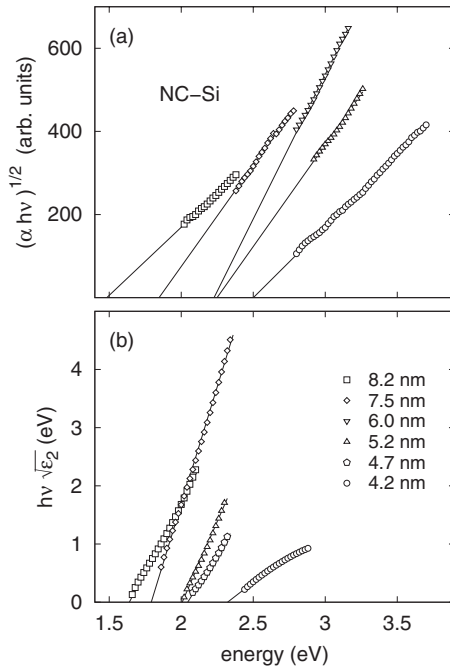
FIG. 3. Tauc-plot representations of optical-absorption measurements: (a) from transmission (b) from ellipsometry. In both cases the fundamental band gap is given by the intersection of the abscissa axis with a linear fit (lines) to the data (symbols).

ing a plot of $h\nu\sqrt{\varepsilon_2}$ vs $h\nu$ (Ref. 14). The linear behavior obtained in Fig. 3(b) is consistent with an indirect character of the fundamental gap and the obtained energy values as function of $d$, although lower, confirm the shift toward higher energies when the NC size decreases. Both sets of results fit the inverse power law: $E_G - E_{Si} = A/d^{\delta}$, where $E_{Si}$ is the band-gap energy of bulk silicon. We find here that $\delta = 1.23 \pm 0.13$. This value shows fair agreement with $\delta = 1.35$, found[16,32] for the "red PL" peak that appears at lower energies than the band gap (see below). Therefore, these two energies, in absorption and in emission, seem to be quite related in the different measurements on our samples.

For the upper gaps, the CP parameters[38] of the $E_1$ and $E_2$ interband transitions were determined very precisely by analyzing the dielectric functions that we obtained. We fitted the numerically built second derivatives, when possible. The results are found to be comparable to the results published by Diebold and Price[13] for nanoslabs. However, the energy shifts measured in our samples are larger and this is in correspondence with the larger variation in the dielectric functions described in Sec. III A. All our results are summarized in Fig. 4. Quantum confinement effects on the upper gaps start to become evident at NC sizes smaller than those for the optical gap because the Bohr radii of excitons associated to higher-energy transitions are also smaller, according to their larger effective masses.

## IV. DISCUSSION AND CONCLUSIONS

Discussing first the details of our ellipsometry results shown in Fig. 2 we note that they consist of two types of
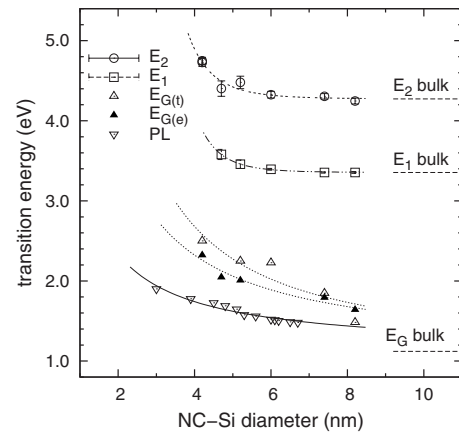


FIG. 4. A summary of the transition energies found in this study as determined from PL, optical transmission, and spectroscopic ellipsometry measurements. The lines are fits with inverse power laws. The values of the transitions in bulk Si crystal are indicated by the horizontal dashed lines.

spectra. At larger NC sizes the nanocrystals display a bulk-like spectrum, although with obvious changes such as an increased absorption below $E_1$ and broader features. It is also obvious that the absorption of the NCs (as seen from the damping of the interference oscillations in Fig. 1), shifts toward the blue when the NC size decreases. To quantify these shifts we have measured the optical transmission and confirmed that the optical gap shifts strongly to higher energies. Then, we found that for the studied range of NC sizes the energies of the upper transitions also show similar variations, as do the PL and the band gap.

Above a NC size of $\sim 5.5$ nm we observe that the dielectric function of the crystallites is *bulklike* with clear $E_1$ and $E_2$ CPs but with larger broadening and reduced amplitudes in comparison with crystalline bulk Si. Below this size, the $E_1$ transition becomes broader and weaker than the $E_2$ transition, tending to disappear. The remaining broad peak related to $E_2$ shifts upwards at smaller sizes. Note that we can only determine $E_2$ down to the 4 nm particle size because of the spectral range limitation of our setup. Comparing with literature data on thin nanoslabs we note that the reductions in $\varepsilon_1$ and in the maximum value of $\varepsilon_2$ are much smaller than those obtained in Si NCs. At the same time, the confinement energies of the interband transitions are also much larger in our case. It appears then that not only the size but also the shape and hence dimensionality of the confined object is a very important parameter in the dispersion of $\varepsilon$, that is, in the density of electronic states. Experimentally, $\varepsilon$ remains bulk-like in nanoslabs down to 3.2 nm thickness[7] but is already quite broad in ultrathin 0.6 nm films composed of disk-shaped patches.[14] In the case of spherical nanoparticles (our case), we have observed that the transition linewidths exhibit a marked increase below 5.5 nm NC size and the reduction in $\varepsilon$ is the largest. Different crystallite shapes mean a change in the ratio of surface-to-volume concentrations of atoms: to have a 0.5 ratio (half of the atoms are in the "bulk" and half are on the "surface") we estimate the following dimensions: a slab (two dimensional) should be around 2 nm thick, a

cylinder (one dimensional) should be 4 nm in diameter, and a sphere (zero dimensional) should be 6 nm in diameter.

Turning to the comprehensive picture of the transition energies that arises from all our spectroscopic results as summarized in Fig. 4, we conclude that the whole band structure shifts to higher energies with the decrease in size of the NCs. In other words, since the shift in all transitions behaves in roughly the same way, the results must be associated with the same QC effect. Moreover, our results show that QC effects are well manifested at least up to NCs of 5.5 nm size. One notes that most of the theoretical works were concerned however, for obvious reasons,[39] with smaller NCs in the sub-3-nm range. We have demonstrated that a complete correlation between the behavior of the optical transitions and the QC effect exists. This, within the accuracy of the present work, is simultaneous, i.e., there is an equal shift of the levels as a function of the crystallites size below 5.5 nm. On the other hand, the PL shifts continuously and concomitantly together with the absorption edge. The PL appears redshifted and this "Stokes"-type shift is very large as is usual in oxide embedded Si NCs.[40] We observe that the Stokes shift shows a tendency to increase with decreasing crystallite size, as described by Wolkin *et al.*[18] but, clearly, in our experiments we are not in the regime of constant level separation and the Wolkin model does not apply, at least in the 4–7 nm range of ensembles of Si NCs embedded in $SiO_2$. However, to account for this observation, we suggest below a model based on the conclusions that we derived above and which is compatible with the various models suggested previously for systems of Si NCs that are embedded in a $SiO_2$ matrix.

In trying to interpret the present results we consider first the four upper curves in Fig. 4. These are the absorption edge transition $E_G$ as well as the transitions $E_1$ and $E_2$ at the corresponding CPs ($\Lambda_3$-$\Lambda_1$ and $X_4$-$X_1$,[38] respectively). Our present results seem to agree with various experimental[41,42] and theoretical[43,44] works that concluded that the basic electronic structure, in particular the indirect nature of the band gap, are maintained, at least in the NCs size range studied here. However, at the same time we have found evidence of the confinement of the valence- and conduction-band states in the nanocrystals. This is a consequence of the relaxation of translational invariance that ultimately leads to the collapse of the entire Brillouin zone of bulk Si into its center point or a three-dimensional folding of all energy bands, giving rise to a series of discrete confined states. The lower-energy transition, $E_G$, is no longer strictly indirect, however, the lowest-energy conduction states still come from "folded" X levels. This transition remains weak and indirect-like because the X states share the same atomic *p*-type character of the top of the valence band[45] and the transition is dipole forbidden. In contrast, L states which in bulk Si lie roughly about 2 eV above the valence-band top[45] have at least 50% *s*-type character, thus, giving rise to optical transitions with substantial oscillator strength. These account for the absorption enhancement between 2 and 3 eV evident in Fig. 2. The growing number of possible transitions is also responsible for the increasing broadening of the spectra.

Considering the PL, we recall our previous conclusions regarding the manifestation of the QC effect on the discrete conduction and valence states $E_c$ and $E_v$ related to the PL process. We have shown previously[32] that whereas $E_c$ shifts as expected from QC theories, the resulting $E_v$ is only weakly dependent on the size of the NCs. The reason for that is that for $E_v$ a strong coupling of the electronic state and the oxide surface vibrations takes place. This effect seems negligible in the $E_c$ case. In passing, we note that the above different behavior of the $E_c$ and $E_v$ levels is not obtained if the mentioned strong coupling is not considered,[46] and in fact our various previous experimental results[32,47] suggest that the effect of the QC on the electrons is much "stronger" than on the holes.

We now turn to the discussion of the relationship between the energies of the absorption edge and the PL (the two lower curves in Fig. 4). There is an intensive debate both on the strong PL (in spite of the weak oscillator strength) (Ref. 42) and on the unusually large "Stokes shift."[40] In particular, we note that whereas a large Stokes shift was reported in many studies, only few of them have attempted to explain it. Basically, these explanations fall into three types. In the first type, it is assumed that the dissipation of the energy of the excited carriers is by optical-phonon emission, that is followed by a radiative transition of the rest of its energy.[19] The second type suggests that the radiative transition is from the band edges to a surface state at the $Si/SiO_2$ encapsulating shell of the crystallites.[24,40,48] In the third type, it is assumed that the excitation itself causes a variation in the local configuration such that the energy associated with the transition is smaller than that associated with the absorption.[49,50] In this context, the redshift may be described as "Franck-Condon-type shift." While our present results cannot provide a conclusive preference to one of these models, they strongly suggest (following the "parallel" behavior of the curves in Fig. 4) that the $E_c$ level is common to absorption and emission. Then, the radiative (PL) transition takes place from $E_c$ to the intermediate level $E_v$ which is different from the level involved in the absorption processes for which no environmental effects need to be considered.[51] It appears to us, then, that combining this conclusion with those of our previous[32] finding (i.e., that $E_c$ shifts as expected from the QC models while $E_v$ hardly varies) for the studied NCs size range, can yield a model that will account for the previous observations and be consistent with the above three types of models as follows. The electrons excited to the $E_c$ dissipate the excess energy by optical phonons that excite the Si-O surface vibration at the NCs surface. This vibration couples with $E_v$ such that the Si-O configuration is changed at the surface of the NCs, on the one hand, and result in the suppression of the nonradiative processes (i.e., the phonon emission) associated with the holes, on the other hand. The "surface state" in that model is the "vibronic" state that we described previously[32] and got theoretical support recently.[52] The high PL intensity, the well-known sensitivity of the PL behavior to the oxidation state of the surface,[19] and the larger Stokes shift for smaller NCs are consistent with this picture.

In conclusion, the main achievements of the present work are the obtention of the dielectric function dispersions and the simultaneous determination of the energies of four

optical transitions as a function of the NCs size in ensembles of Si NCs embedded in a $SiO_2$ matrix. This relied on an independent and explicit determination of the sizes of the NCs that was used for the investigation of the present optical spectroscopy measurements. The conspicuous result of this study is that the same semiquantitative quantum confinement behavior accounts for all four transitions. Hence, although the PL process is much more susceptible to surface effects in Si NCs, it follows simply the QC-controlled absorption processes. This, in turn, sheds some light into the problem of explaining the very large Stokes-type shift observed between PL and the absorption edge in a variety of Si-$SiO_2$ nanocomposites.

*isabel.alonso@icmab.es

[1] D. Amans, S. Callard, A. Gagnaire, J. Joseph, G. Ledoux, and F. Huisken, J. Appl. Phys. **93**, 4173 (2003).

[2] M. Losurdo, M. M. Giangregorio, P. Capezzuto, G. Bruno, M. F. Cerqueira, E. Alves, and M. Stepikhova, Appl. Phys. Lett. **82**, 2993 (2003).

[3] K. H. Jun, S. J. Baik, K. S. Lim, H. S. Lee, and J. Y. Lee, Phys. Rev. B **67**, 155326 (2003).

[4] J. A. Moreno, B. Garrido, P. Pellegrino, C. Garcia, J. Arbiol, J. R. Morante, P. Marie, F. Gourbilleau, and R. Rizk, J. Appl. Phys. **98**, 013523 (2005).

[5] M. H. Khatun, M. Shahjahan, R. Ito, K. Sawada, and M. Ishida, Thin Solid Films **508**, 65 (2006).

[6] R. C. Mani, I. Pavel, and E. S. Aydil, J. Appl. Phys. **102**, 043305 (2007).

[7] H. G. Yoo and P. M. Fauchet, Phys. Rev. B **77**, 115355 (2008).

[8] S. K. Ram, M. N. Islam, P. R. I. Cabarrocas, and S. Kumar, Thin Solid Films **516**, 6863 (2008).

[9] Y. Bouizem, C. Abbes, J. D. Sib, D. Benlakehal, R. Baghdad, L. Chahed, K. Zellama, and S. Charvet, J. Phys.: Condens. Matter **20**, 445221 (2008).

[10] L. Ding, T. P. Chen, Y. Liu, C. Y. Ng, Y. C. Liu, and S. Fung, Appl. Phys. Lett. **87**, 121903 (2005).

[11] A. Szekeres, T. Nikolova, A. Paneva, I. Lisovskyy, P. E. Shepeliavyi, and G. Y. Rudko, Opt. Mater. **30**, 1115 (2008).

[12] M. Mansour, A. E. Naciri, L. Johann, J. J. Grob, and M. Stchakovsky, Phys. Status Solidi A **205**, 845 (2008).

[13] A. C. Diebold and J. Price, Phys. Status Solidi A **205**, 896 (2008).

[14] H. V. Nguyen, Y. Lu, S. Kim, M. Wakagi, and R. W. Collins, Phys. Rev. Lett. **74**, 3880 (1995).

[15] I. Stenger, B. Gallas, L. Siozade, C.-C. Kao, S. Chenot, S. Fisson, G. Vuye, and J. Rivory, J. Appl. Phys. **103**, 114303 (2008).

[16] A. Sa'ar, J. Nanophotonics **3**, 032501 (2009).

[17] S. V. Gaponenko, *Optical Properties of Semiconductor Nanocrystals*, Cambridge Studies in Modern Optics Vol. 23 (Cambridge University Press, Cambridge, UK, 1998).

[18] M. V. Wolkin, J. Jorne, P. M. Fauchet, G. Allan, and C. Delerue, Phys. Rev. Lett. **82**, 197 (1999).

[19] S. Godefroo, M. Hayne, M. Jivanescu, A. Stesmans, M. Zacharias, O. I. Lebedev, G. Van Tendeloo, and V. V. Moshchalkov, Nat. Nanotechnol. **3**, 174 (2008).

[20] N. Daldosso and L. Pavesi, in *Nanosilicon*, edited by V. Kumar (Elsevier, New York, 2008), p. 314.

[21] B. Gallas, I. Stenger, C.-C. Kao, S. Fisson, G. Vuye, and J. Rivory, Phys. Rev. B **72**, 155319 (2005).

[22] L. Ding, T. P. Chen, Y. Liu, M. Yang, J. I. Wong, Y. C. Liu, A. D. Trigg, F. R. Zhu, M. C. Tan, and S. Fung, J. Appl. Phys. **101**, 103525 (2007).

[23] L.-W. Wang and A. Zunger, Phys. Rev. Lett. **73**, 1039 (1994).

[24] J. P. Wilcoxon, G. A. Samara, and P. N. Provencio, Phys. Rev. B **60**, 2704 (1999).

[25] C. S. Garoufalis, A. D. Zdetsis, and S. Grimme, Phys. Rev. Lett. **87**, 276402 (2001).

[26] M. Dovrat, Y. Goshen, J. Jedrzejewski, I. Balberg, and A. Sa'ar, Phys. Rev. B **69**, 155311 (2004).

[27] A. N. Karpov, D. V. Marin, V. A. Volodin, J. Jedrzejewski, G. A. Kachurin, E. Savir, N. L. Shwartz, Z. S. Yanovitskaya, I. Balberg, and Y. Goldstein, Semiconductors **42**, 731 (2008).

[28] A. Sa'ar, M. Dovrat, J. Jedrzejewski, I. Popov, and I. Balberg, Phys. Status Solidi A **204**, 1491 (2007).

[29] I. V. Antonova, M. Gulyaev, E. Savir, J. Jedrzejewski, and I. Balberg, Phys. Rev. B **77**, 125318 (2008).

[30] J. J. Hanak, J. Mater. Sci. **5**, 964 (1970).

[31] B. Abeles, P. Sheng, M. D. Coutts, and Y. Arie, Adv. Phys. **24**, 407 (1975).

[32] A. Sa'ar, Y. Reichman, M. Dovrat, D. Krapf, J. Jedrzejewski, and I. Balberg, Nano Lett. **5**, 2443 (2005).

[33] M. Garriga, M. I. Alonso, and C. Domínguez, Phys. Status Solidi B **215**, 247 (1999).

[34] M. Garriga, M. Cardona, N. E. Christensen, P. Lautenschlager, T. Isu, and K. Ploog, Phys. Rev. B **36**, 3254 (1987).

[35] D. E. Aspnes, J. B. Theeten, and F. Hottier, Phys. Rev. B **20**, 3292 (1979).

[36] T. W. Noh, P. H. Song, and A. J. Sievers, Phys. Rev. B **44**, 5459 (1991).

[37] B. Gallas, C.-C. Kao, C. Defranoux, S. Fisson, G. Vuye, and J. Rivory, Thin Solid Films **455-456**, 335 (2004).

[38] P. Lautenschlager, M. Garriga, L. Viña, and M. Cardona, Phys. Rev. B **36**, 4821 (1987).

[39] L. E. Ramos, H. C. Weissker, J. Furthmuller, and F. Bechstedt, Phys. Status Solidi B **242**, 3053 (2005).

[40] Y. Kanemitsu and S. Okamoto, Phys. Rev. B **58**, 9652 (1998).

[41] T. Matsumoto, J. I. Suzuki, M. Ohnuma, Y. Kanemitsu, and Y.

Masumoto, Phys. Rev. B **63**, 195322 (2001).

[42] D. Kovalev, H. Heckler, G. Polisski, J. Diener, and F. Koch, Opt. Mater. **17**, 35 (2001).

[43] C. Delerue, G. Allan, C. Reynaud, O. Guillois, G. Ledoux, and F. Huisken, Phys. Rev. B **73**, 235318 (2006).

[44] F. Trani, D. Ninno, and G. Iadonisi, Phys. Rev. B **76**, 085326 (2007).

[45] M. L. Cohen and J. R. Chelikowsky, *Electronic Structure and Optical Properties of Semiconductors*, Springer Series in Solid-State Sciences Vol. 75 (Springer-Verlag, Berlin, 1988), p. 81.

[46] N. A. Hill and K. B. Whaley, Phys. Rev. Lett. **75**, 1130 (1995).

[47] H. L. Aharoni, D. Azulay, O. Millo, and I. Balberg, Appl. Phys. Lett. **92**, 112109 (2008).

[48] K. Murayama, H. Komatsu, S. Miyazaki, and M. Hirose, J. Non-Cryst. Solids **198-200**, 953 (1996).

[49] E. Degoli, G. Cantele, E. Luppi, R. Magri, D. Ninno, O. Bisi, and S. Ossicini, Phys. Rev. B **69**, 155411 (2004).

[50] L. K. Pan, Z. Sun, and C. Q. Sun, Scr. Mater. **60**, 1105 (2009).

[51] X. L. Wu, S. J. Xiong, D. L. Fan, Y. Gu, X. M. Bao, G. G. Siu, and M. J. Stokes, Phys. Rev. B **62**, R7759 (2000).

[52] M. Mahdouani, R. Bourguiga, and S. Jaziri, Physica E **41**, 228 (2008).